Equilibrium and Stability of Field-Reversed Configurations with Toroidal Field

Yu. A. Omelchenko, M. Schaffer, P. Parks

General Atomics
P.O. Box 85608, San Diego, California 92186-5608

42st APS Annual APS Meeting of the Division of Plasma Physics
Québec City, October 23-28, 2000.

Abstract

- The Field-Reversed Configuration (FRC) is a high-beta compact toroidal plasma in which the external field is reversed on axis by azimuthal plasma current.
- The FRC is primarily confined by poloidal fields. The possibility of the presence of self-generated toroidal field inside the separatrix has been largely ignored in the previous stability analysis of such configurations. Those studies have not identified a physical mechanism that would explain the robust tilt stability of experimentally produced FRCs.
- Recent FRC formation and stability simulations [1] performed with a 3-D, hybrid, PIC code FLAME [2] for a limited set of toroidal modes ($m = 0, 1$) revealed the important role of toroidal field effects in mitigating FRC tilting.
- Here we shift focus to demonstrating the enhanced stability of the FRCs with toroidal fluxes to a number of kink modes, including the most disruptive tilt mode.

GENERAL ATOMICS

Introduction

- The FRC kink instability (including the m=1 tilt) has been studied in both MHD and kinetic regimes under the assumption of no toroidal self-field inside the separatrix.
- MHD theory predicts FRC confinement degradation and destruction on the Alfven timescale. Stabilization by profile shaping has been shown to be eventually ineffective [3].
- Kinetic simulations of FRC stability employ hybrid schemes but traditionally use a single-fluid Grad-Shafranov equilibrium (assuming $B_\theta = 0$) as a starting point [4]. These studies focus only on the kinetic effects resulting predominantly from large orbit phase mixing.
- This work examines the importance of the Hall term normally ignored in the MHD description. This is the most significant mechanism in generating toroidal self-field in FRC-like compact toroids (CTs) as shown both in theoretical [5],[1] and experimental [6],[7] studies.

Simulation Model

FLAME is a hybrid, PIC code created to simulate plasma phenomena in the 3-D, cylindrical (r, θ, z) geometry. It follows low-frequency, quasi-neutral plasma motions described by the Maxwell equations in the Darwin approximation:

$$\frac{\partial \mathbf{B}}{\partial t} = -c\nabla \times \mathbf{E}, \quad \nabla \times \mathbf{B} = \frac{4\pi}{c}(\mathbf{j}_e + \mathbf{j}_i) \tag{1}$$

Multiple ion species are represented by full-orbit macro-particles and the plasma electrons are modeled as a massless collisional fluid (Ohm's law):

$$\mathbf{E} = \eta \mathbf{j}_e + \frac{\mathbf{j}_e \times \mathbf{B}}{en_e c} - \frac{\nabla p_e}{en_e}, \quad \eta = \frac{4\pi(\nu_{ei} + \nu_{en})}{\omega_{pe}^2}. \tag{2}$$

$$\frac{1}{\gamma - 1}\frac{\partial p_e}{\partial t} = -\frac{1}{\gamma - 1}\nabla(p_e \mathbf{v}_e) - p_e \nabla \mathbf{v}_e + Q_e, \quad Q_e = \eta \mathbf{j}_e^2. \tag{3}$$

In this work we ignore the electron thermal effects ($p_e = 0$).

GENERAL ATOMICS

B_θ-Generation $(\partial/\partial\theta = 0)$

$$\frac{\partial B_\theta}{\partial t} = -\hat{\theta}\cdot\nabla\times\frac{1}{en_e}\left[(\frac{c}{4\pi}\nabla\times\mathbf{B}-\mathbf{j}_i)\times\mathbf{B}-c\nabla p_e\right] \tag{4}$$

In the axisymmetric case $(\eta = 0,\ \mathbf{B} = \nabla\psi\times\nabla\theta + I_\theta\nabla\theta, I_\theta = rB_\theta)$ there are several physical drivers of B_θ, i.e. the Hall effect (nonuniform poloidal $\mathbf{B}$), nonlinear terms and ion/electron thermal effects:

$$\frac{\partial I_\theta}{\partial t} = r^2\left[\psi, \frac{\nabla_*\psi}{n_e r^2}\right] + r^2\left[rI_\theta, \frac{I_\theta}{n_e r^2}\right] + S_{i\theta} + S_{e\theta} \tag{5}$$

where

$$[X, Y] = (\nabla X\times\nabla\theta)\cdot\nabla Y, \quad \nabla_* = \nabla^2 - 2\partial/r\partial r \tag{6}$$

The predominant mechanism in generating B_θ is through the Hall term. It scales as

$$\frac{v_{Hall}}{v_A} \simeq \frac{cB}{4\pi enRv_A} \sim \frac{c/\omega_{pi}}{R} \simeq \frac{r_{ci}}{R} \tag{7}$$

The electron pressure effect is small: $S_{e\theta} \sim \hat{\theta}\cdot(\nabla n_e\times\nabla T_e) \sim 0.$

FRC Formation Setup

- Axisymmetric FRCs with different values of parameter s^* (the number of ion gyroradii between the O-point and the separatrix) are formed by applying a new numerical technique :
  1. Initialize a distribution of ion macro-particles with uniform temperature and density profiles.
  2. Apply an external electric field in the θ-direction. Run the code until the field reversal on axis takes place.
  3. Turn off the applied electric field, decrease the plasma resistivity and run the code until an approximate equilibrium is reached.
- FRCs obtained in this work are similar to ones produced by simulating an imploding θ-pinch discharge [1]. The FRC parameters used in this study are summarized in Table 1.
- FRCs with the same s^* are generated twice: (1) by imposing $B_\theta = 0$; (2) by solving the model equations self-consistently.

GENERAL ATOMICS

3-D FRC Equilibrium Setup

- Axisymmetric FRCs are projected into 3-D space by distributing the field and particle inventory uniformly in the θ-dimension. The $m \leq 4$ toroidal modes are currently enabled in the system.
- An initial $m = 1$ perturbation is applied to ion axial velocities (of order $0.02 v_A$). Its amplitude is chosen to be proportional to ψ^2 (it vanishes at the separatrix, $\psi = 0$).
- The purpose of this study is twofold:
  1. The simulation is run long enough to demonstrate nonlinear saturation of initially unstable kink modes.
  2. Each self-consistent stability run is accompanied by a "reduced" simulation with $B_\theta = 0$. The comparative analysis of these runs is helpful in understanding the role of B_θ in preventing rapid FRC termination.

Table 1 (Summary of FRC Runs)

Run	$s^* = 4$	$s^* = 10$
Wall Radius	15 cm	15 cm
Background $\mathbf{B_z}$	1.8 kG	5 kG
Peak Density	10^{15} cm^{-3}	0.57×10^{16} cm^{-3}
Ion Temperature	160 eV	200 eV
Separatrix Length	40 cm	40 cm
Separatrix Radius	10.5 cm	10 cm
O-Point Radius	7.5 cm	7 cm
Elongation	2	2
Ion Gyroradius	0.7 cm	0.3 cm
Alfven Velocity	1.25×10^7 cm/s	1.5×10^7 cm/s
MHD Growth Time	1.6 μs	1.3 μs
Grid Size $(\mathbf{z}, \mathbf{r}, \mathbf{m})$	$80 \times 40 \times 4$	$80 \times 40 \times 4$
$\mathbf{N_{PIC}}$ (3-D)	$700,000$	$700,000$

FRC Global Stability I (Theory)

- We focus on the enhanced stability properties of FRC-like configurations with a certain amount of toroidal field generated during the FRC formation.
- The most significant effect in generating toroidal field is the Hall effect. In terms of the MHD energy principle this corresponds to adding another stabilizing field-bending term to the energy equation.
- Since the Hall term tends to bend field lines predominantly in the toroidal direction (in contrast to Alfven-driven plasma motion), this does not result in increasing poloidal field curvature. Therefore, this effect is always stabilizing.
- The magnitude of the Hall effect scales as r_{ci}/R (R is the characteristic magnetic gradient length). Thus, the self-generated toroidal field should be an important stabilizing factor in low-s (kinetic) plasmas.
- We also explore stability properties of "fusion-scale" FRCs ($s^* \sim 10$).

FRC Global Stability II (Results)

- All simulations have been run long enough to demonstrate the nonlinear saturation of the kink/tilt instability through kinetic phase mixing and FRC shape relaxation.
- As shown in Fig. 1(a,b) the low-s self-consistent FRC does not exhibit significant confinement degradation during the instability.
- Fig. 2(a,b) illustrates the dynamics of the "zero-B_θ" kinetic FRC. Its internal poloidal structure undergoes more deformation compared to the self-consistent run. Time histories of magnetic field modes (Fig. 5(a,b,c)) corraborate this finding.
- The "fluid-like" FRCs are shown in Fig. 3(a,b,c) and Fig. 4(a,b). The self-consistent FRC is still more robust in conserving its poloidal flux.
- In all cases the kinks are stabilized by virtue of ion phase mixing in the toroidal dimension and FRC plasma axial expansion (Fig. 7).

Conclusion

- The kink modes are the most disruptive toroidal modes that can cause rapid FRC confinement degradation. The ideal MHD theory predicts fast FRC termination. On the contrary, this study demonstrates the FRC robustness with respect to generating such modes, including the most feared tilt mode.
- The FRC tilt stabilization is achieved through nonlinear kinetic ion motion (toroidal phase mixing) resulting in an FRC plasma relaxation in the poloidal plane and expansion in the axial direction.
- The tilt-driven confinement degradation is effectively prevented in the low-s FRC and reduced in the high-s case by virtue of toroidal self-field generation (the Hall term effect), which increases the CT local helicity without destabilizing bad field curvature regions.
- The results of this study are in good agreement with available experimental evidence of robust kinetic FRC stability and existence of toroidal fluxes in the FRC-like configurations.

GENERAL ATOMICS

Figure 1a: Poloidal Flux ($s^* = 4$, $B_\theta \neq 0$)

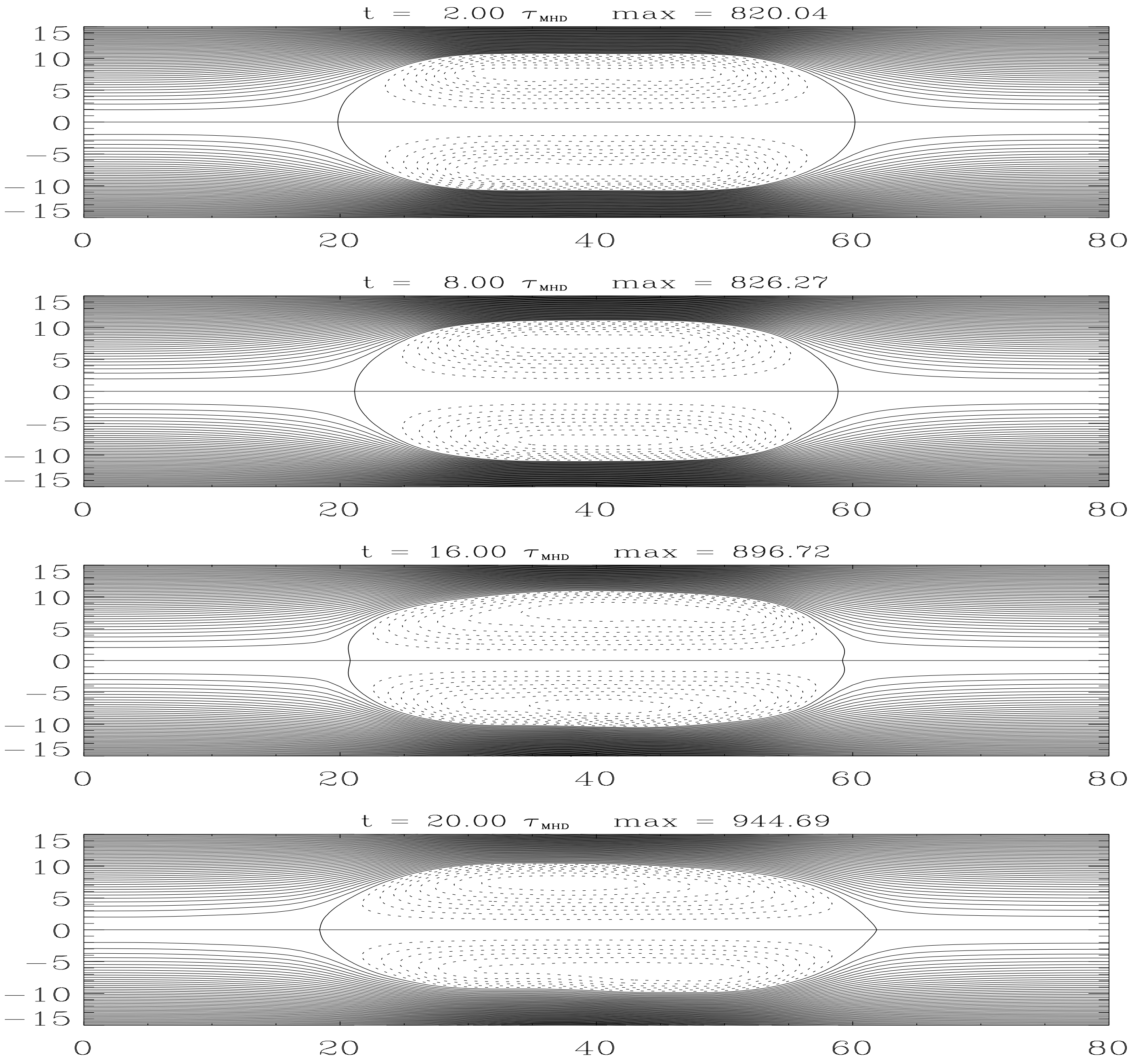

Figure 1b: Plasma Density ($s^* = 4$, $B_\theta \neq 0$)

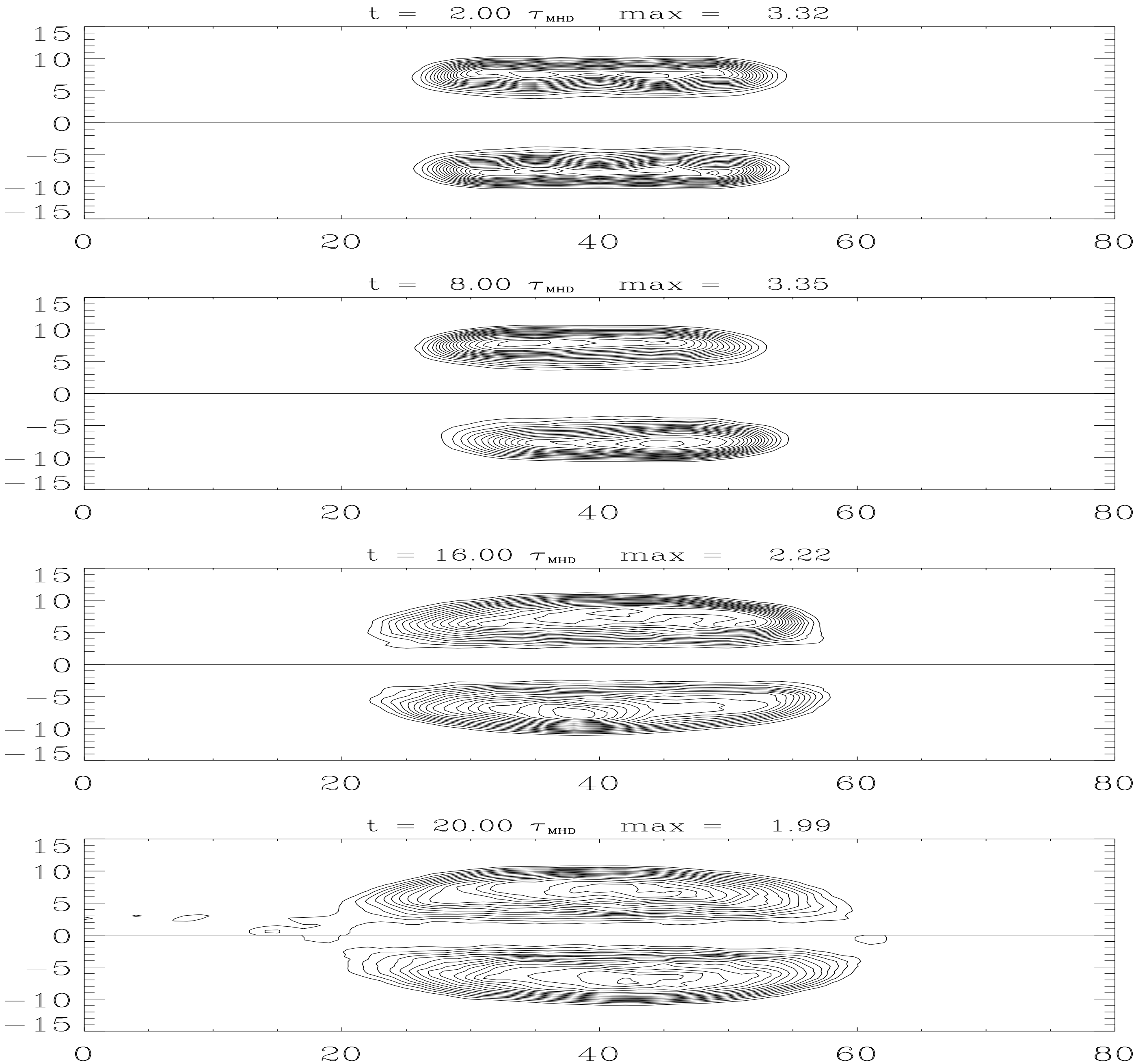

Figure 1c: Toroidal Field ($s^* = 4$, $B_\theta \neq 0$)

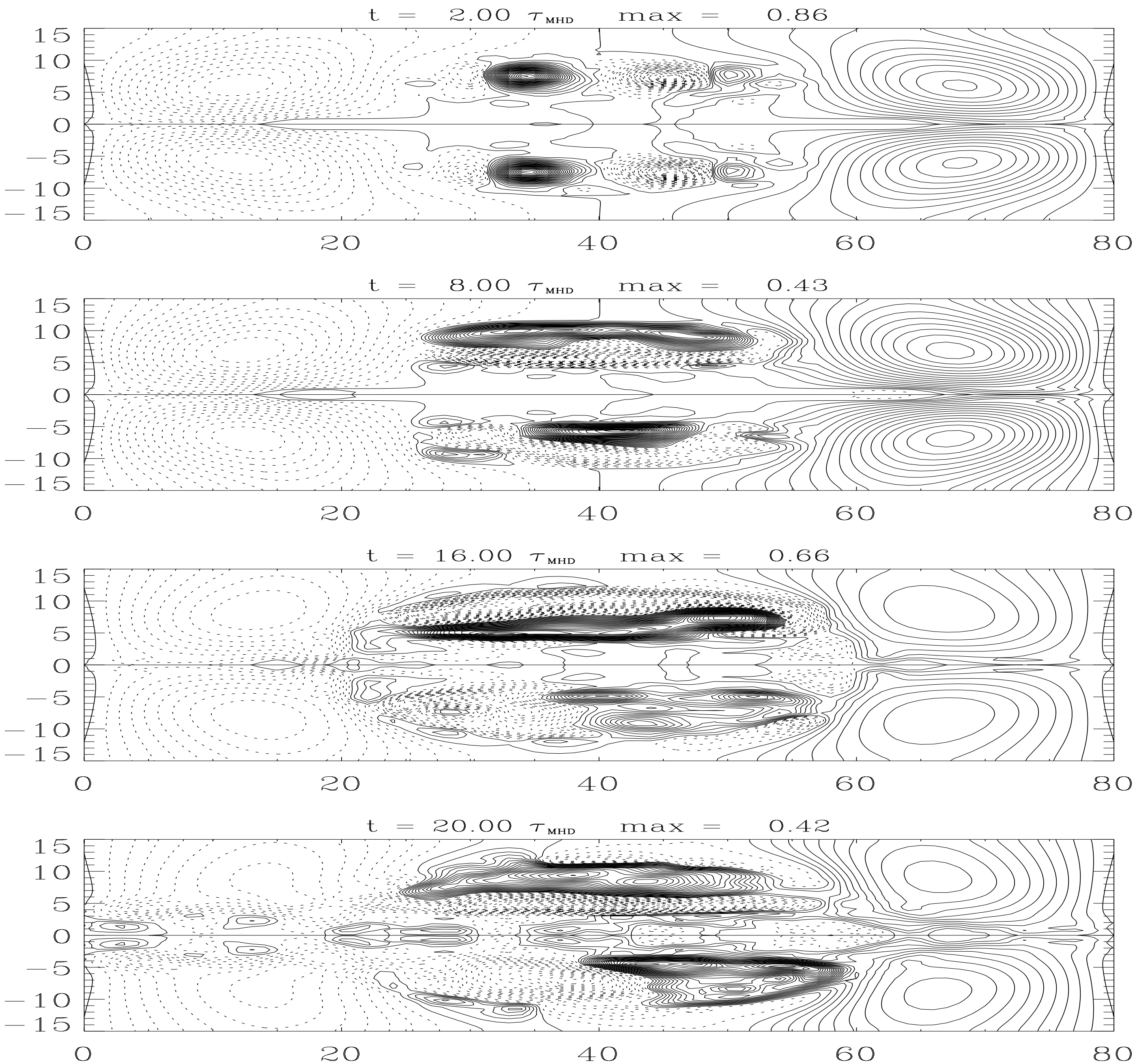

Figure 2a: Poloidal Flux $(s^* = 4,\ B_\theta = 0)$

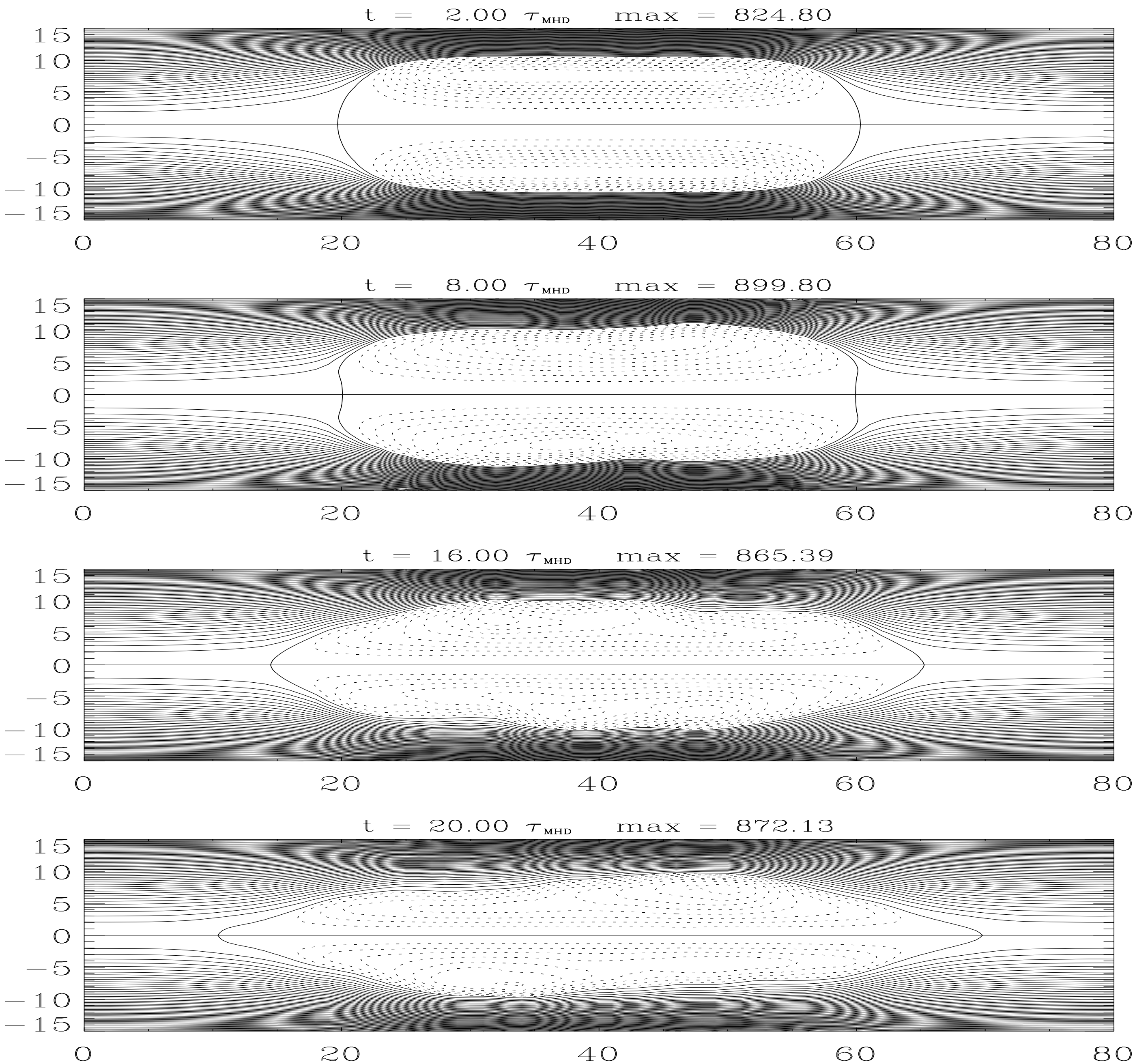

Figure 2b: Plasma Density ($s^* = 4$, $B_\theta = 0$)

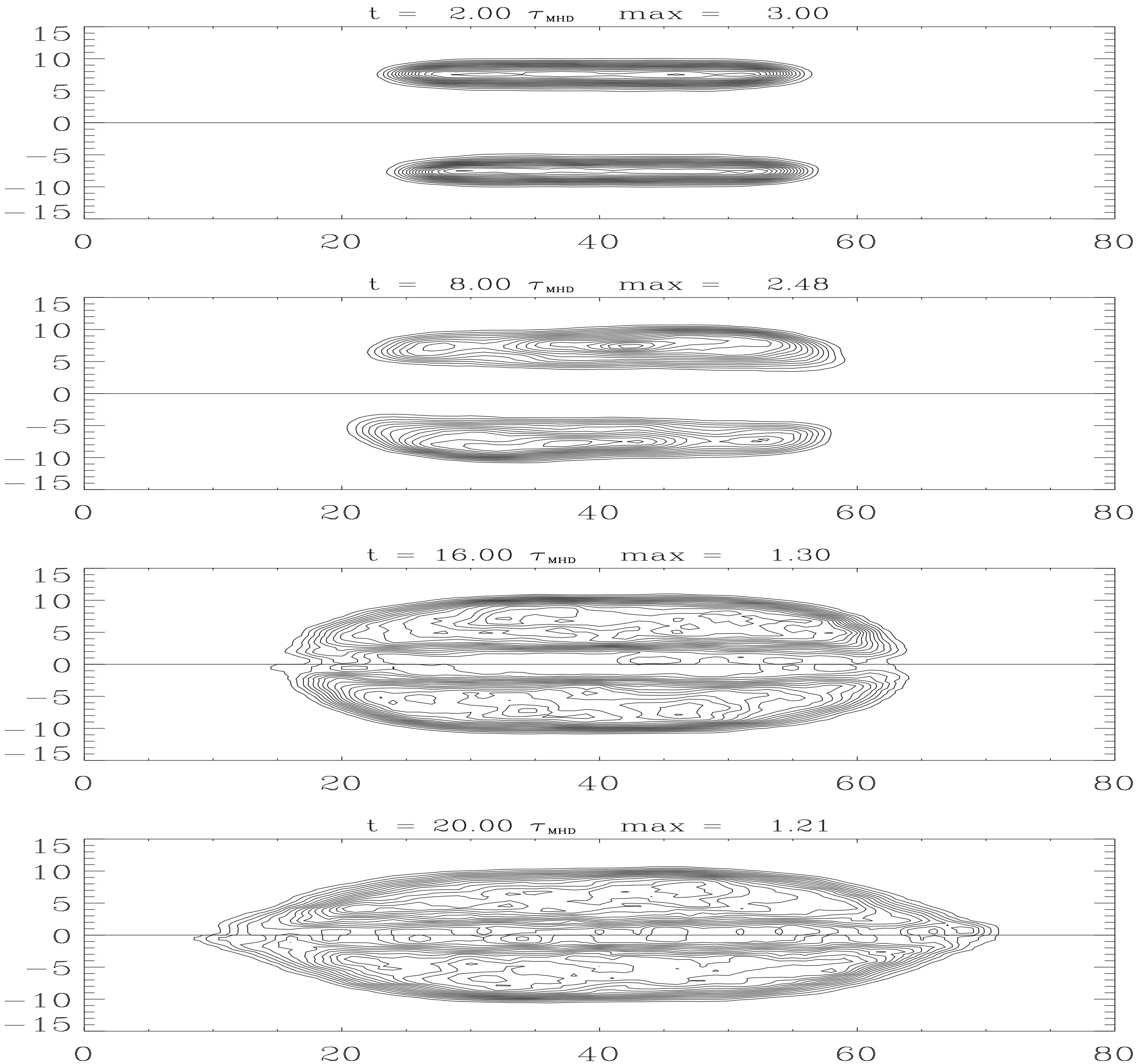

Figure 3a: Poloidal Flux ($s^* = 10,\ B_\theta \neq 0$)

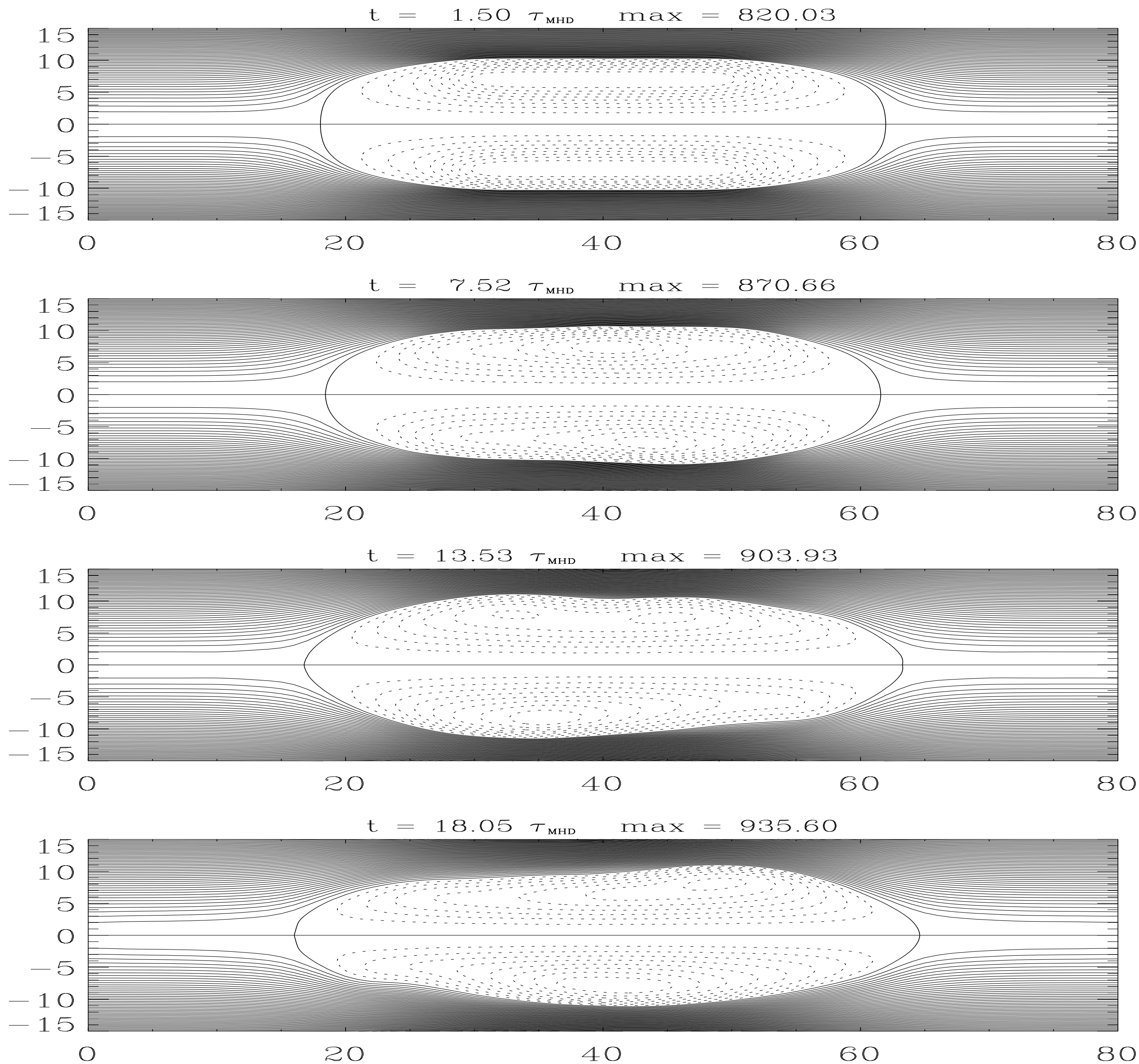

Figure 3b: Plasma Density ($s^* = 10$, $B_\theta \neq 0$)

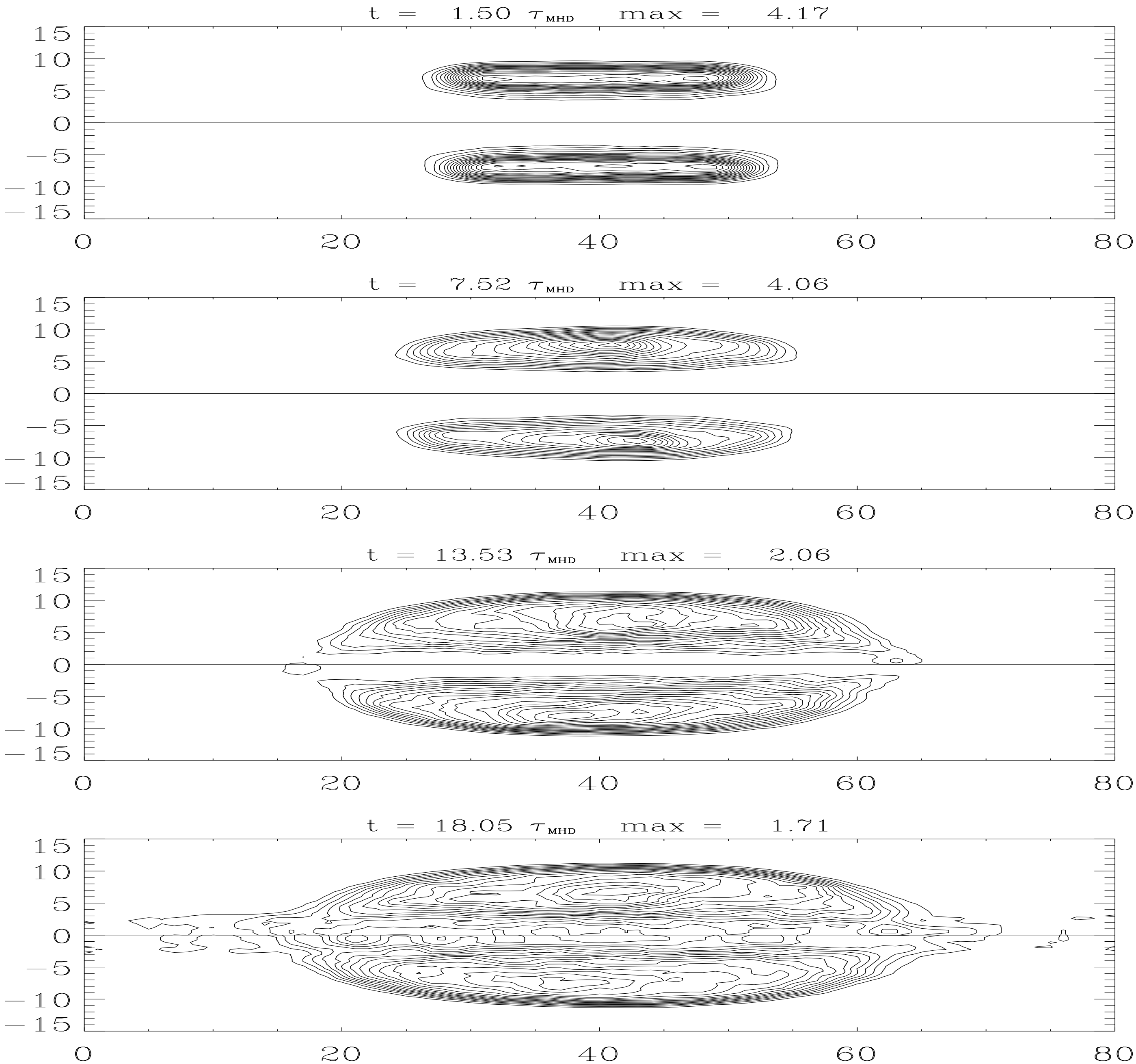

Figure 3c: Toroidal Field ($s^* = 10$, $B_\theta \neq 0$)

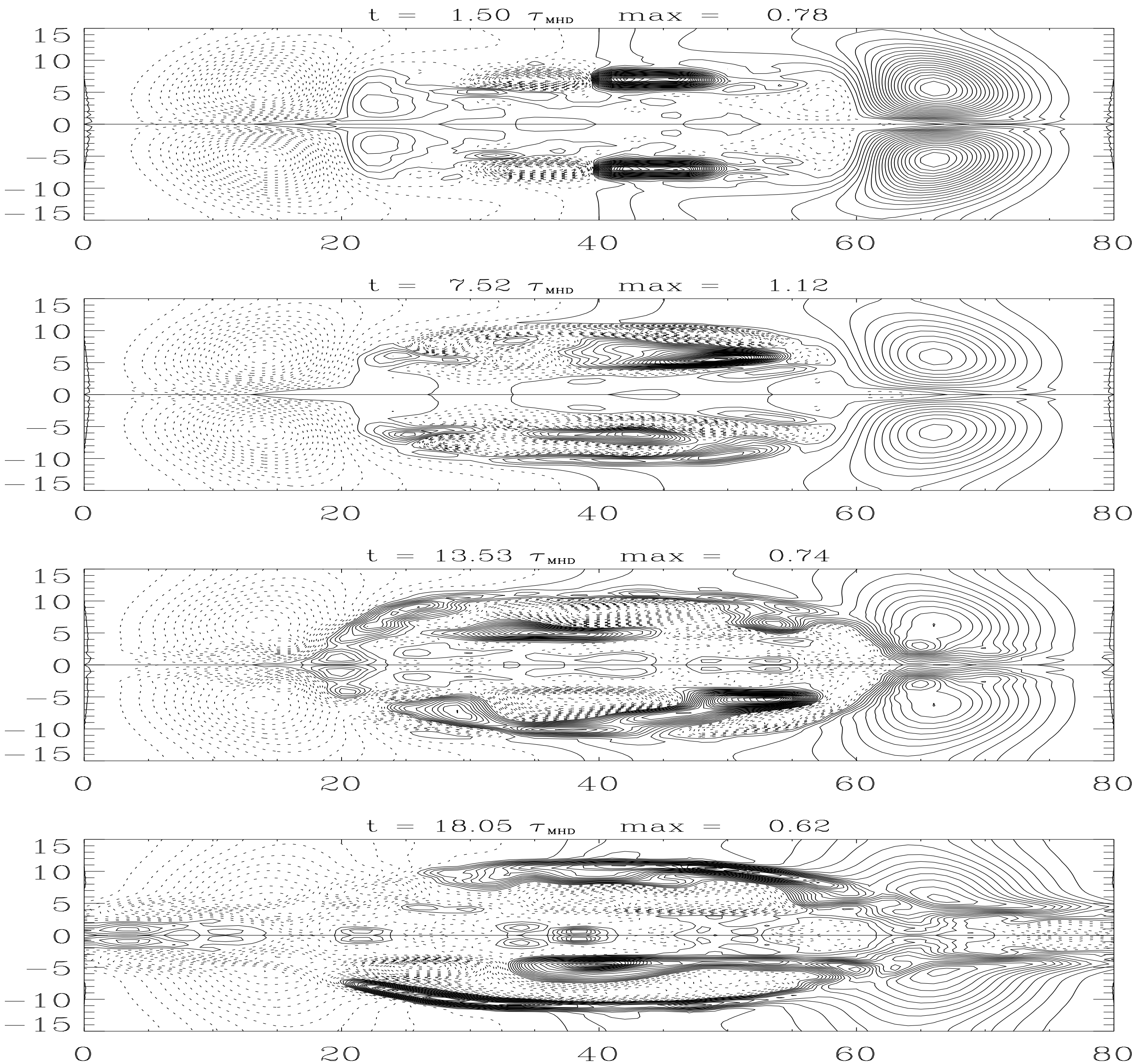

Figure 4a: Poloidal Flux ($s^* = 10$, $B_\theta = 0$)

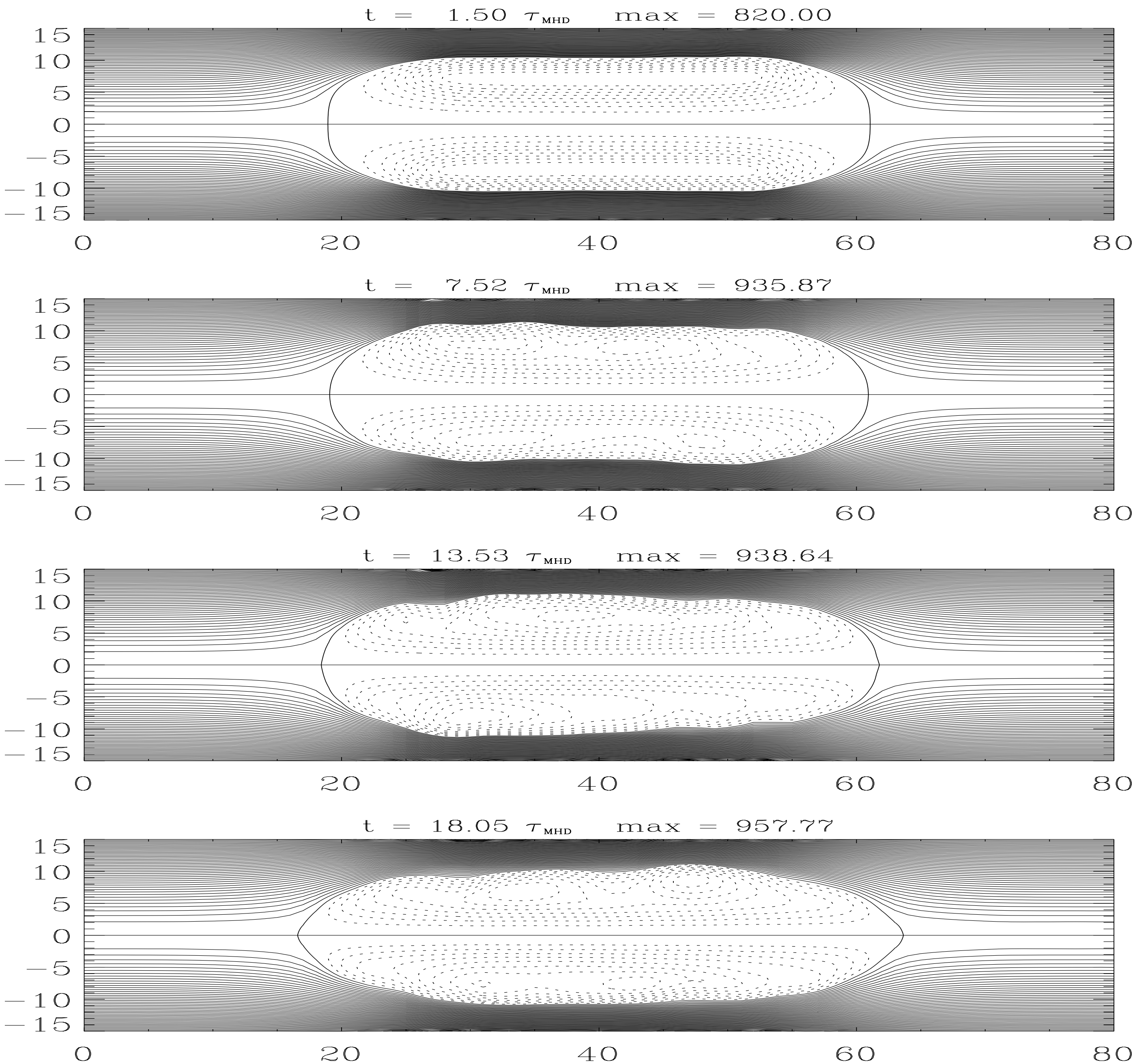

Figure 4b: Plasma Density ($s^* = 10$, $B_\theta = 0$)

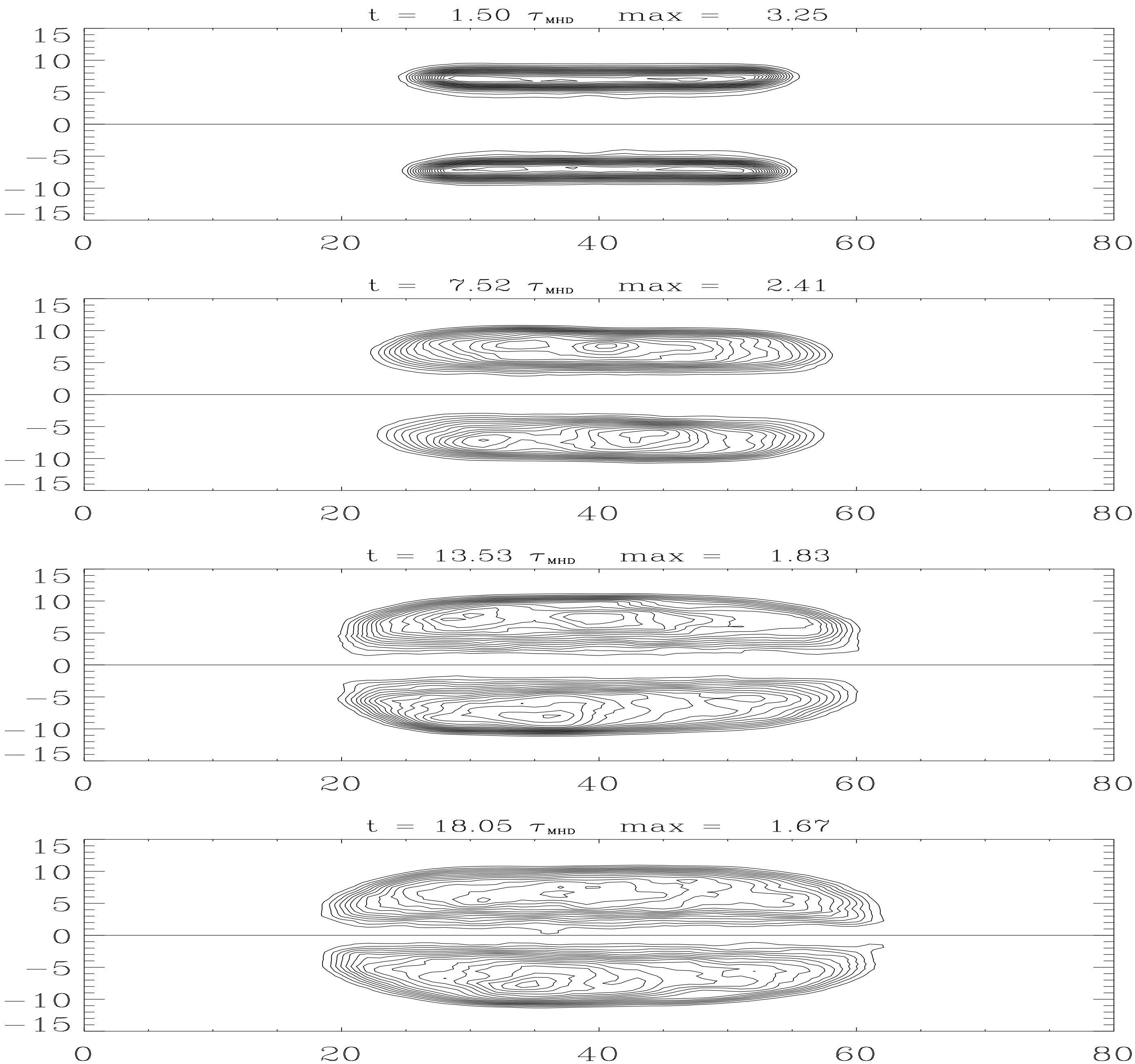

Figure 5a: Mode Evolution ($s^* = 4$, $B_\theta \neq 0$)

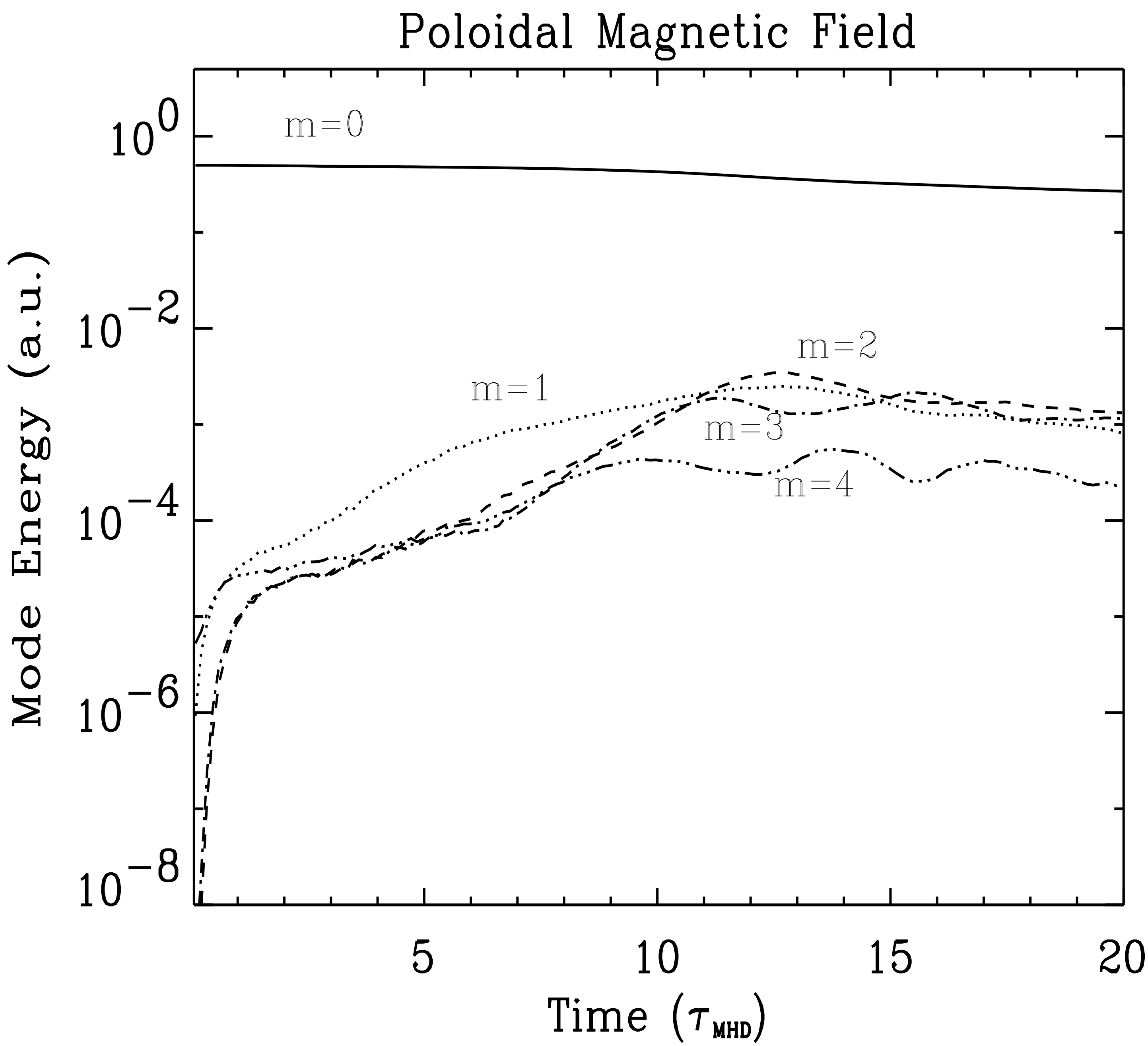

Figure 5b: Mode Evolution ($s^* = 4$, $B_\theta \neq 0$)

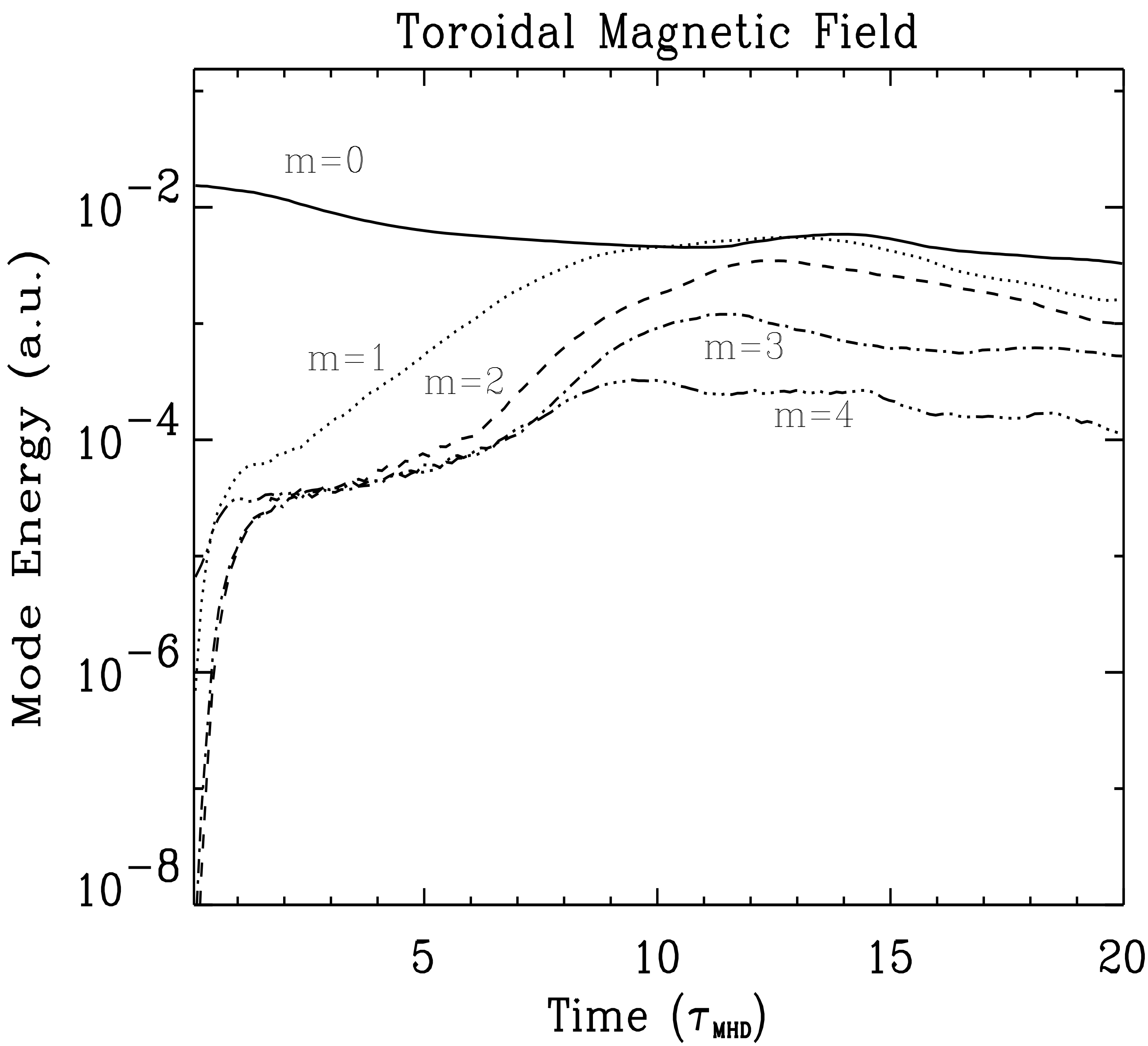

Figure 5c: Mode Evolution ($s^* = 4$, $B_\theta = 0$)

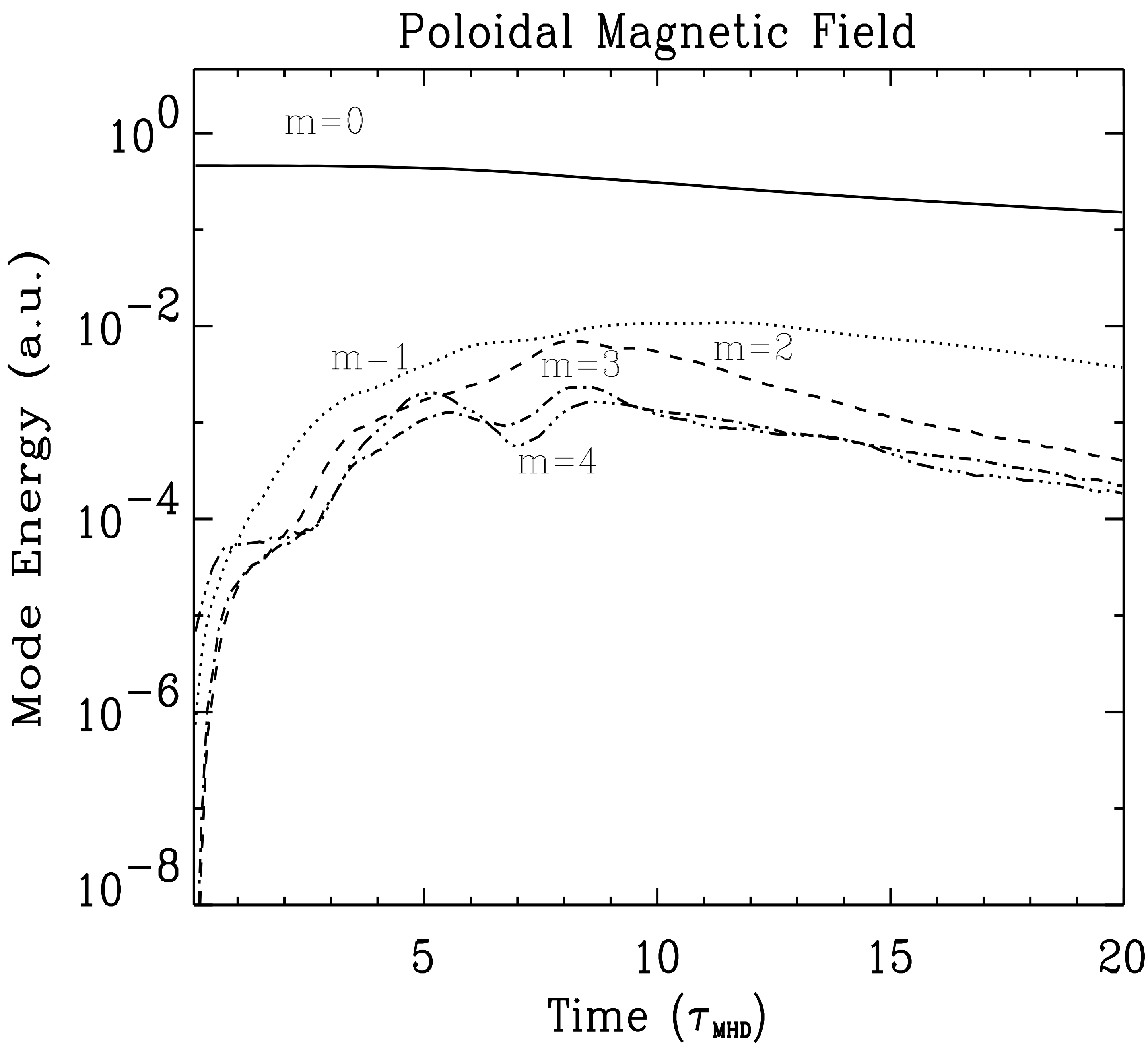

Figure 6a: Mode Evolution ($s^* = 10$, $B_\theta \neq 0$)

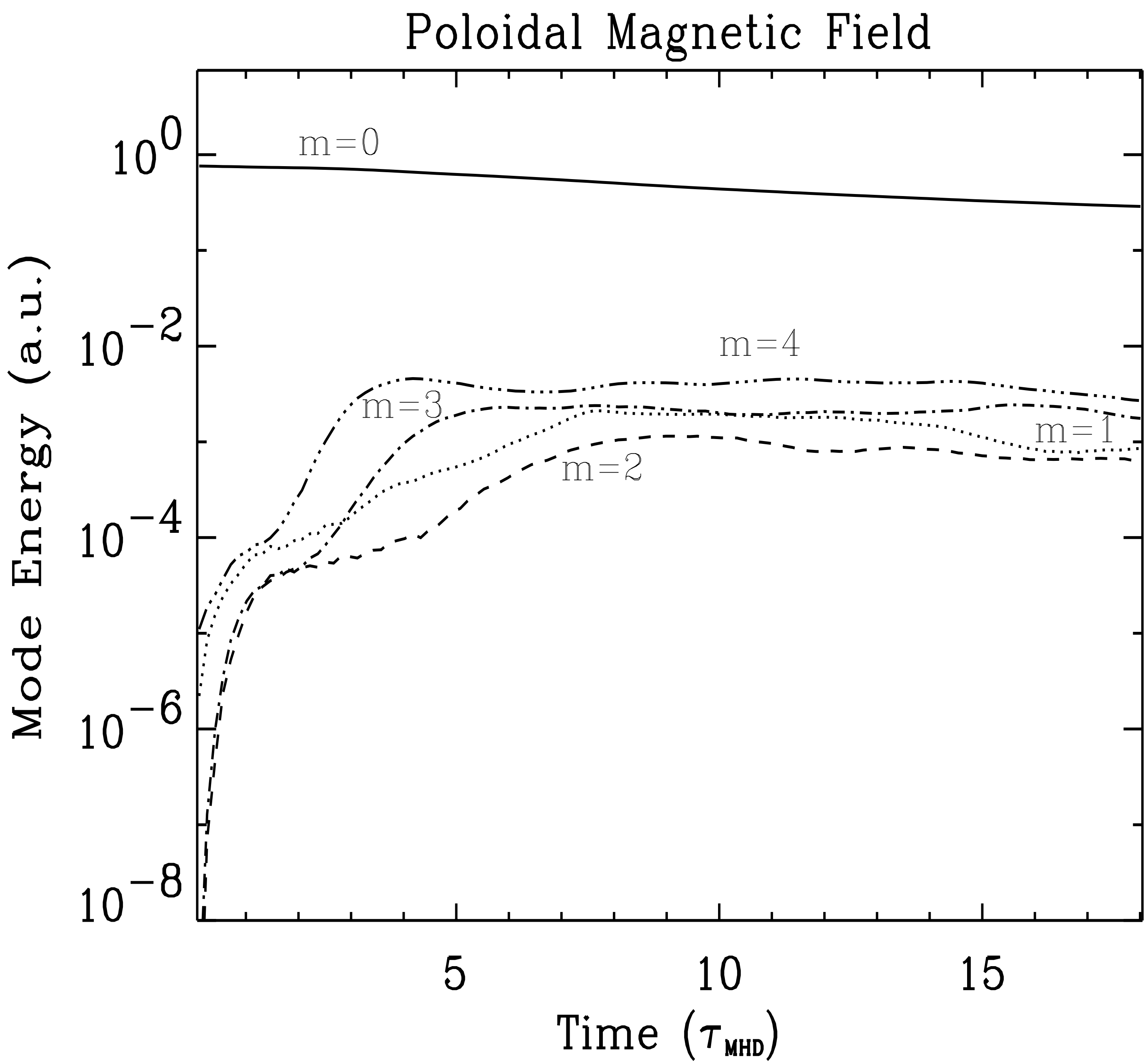

Figure 6b: Mode Evolution ($s^* = 10$, $B_\theta \neq 0$)

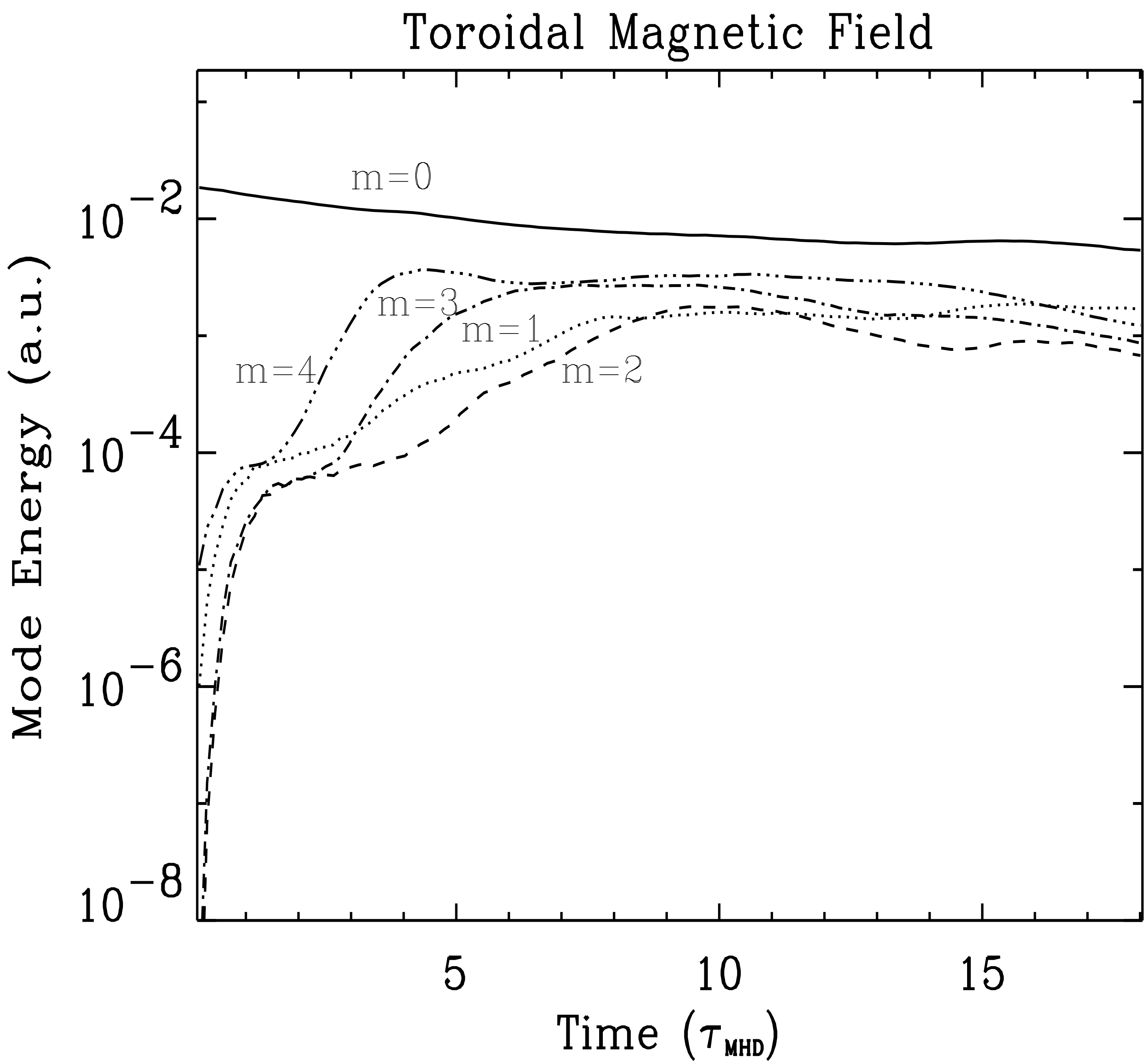

Figure 6c: Mode Evolution ($s^* = 10,\ B_\theta = 0$)

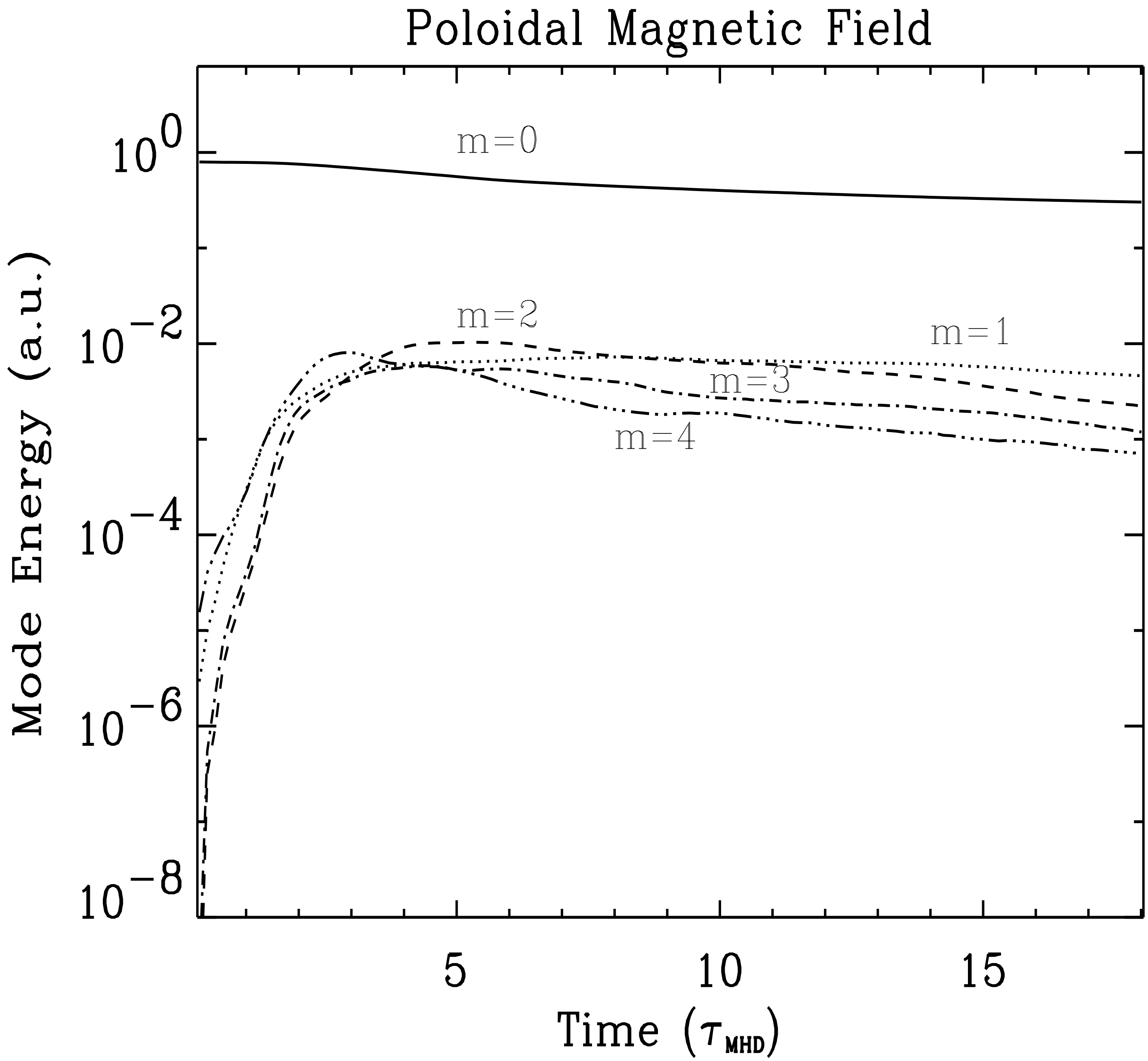

Figure 7: FRC Axial Expansion

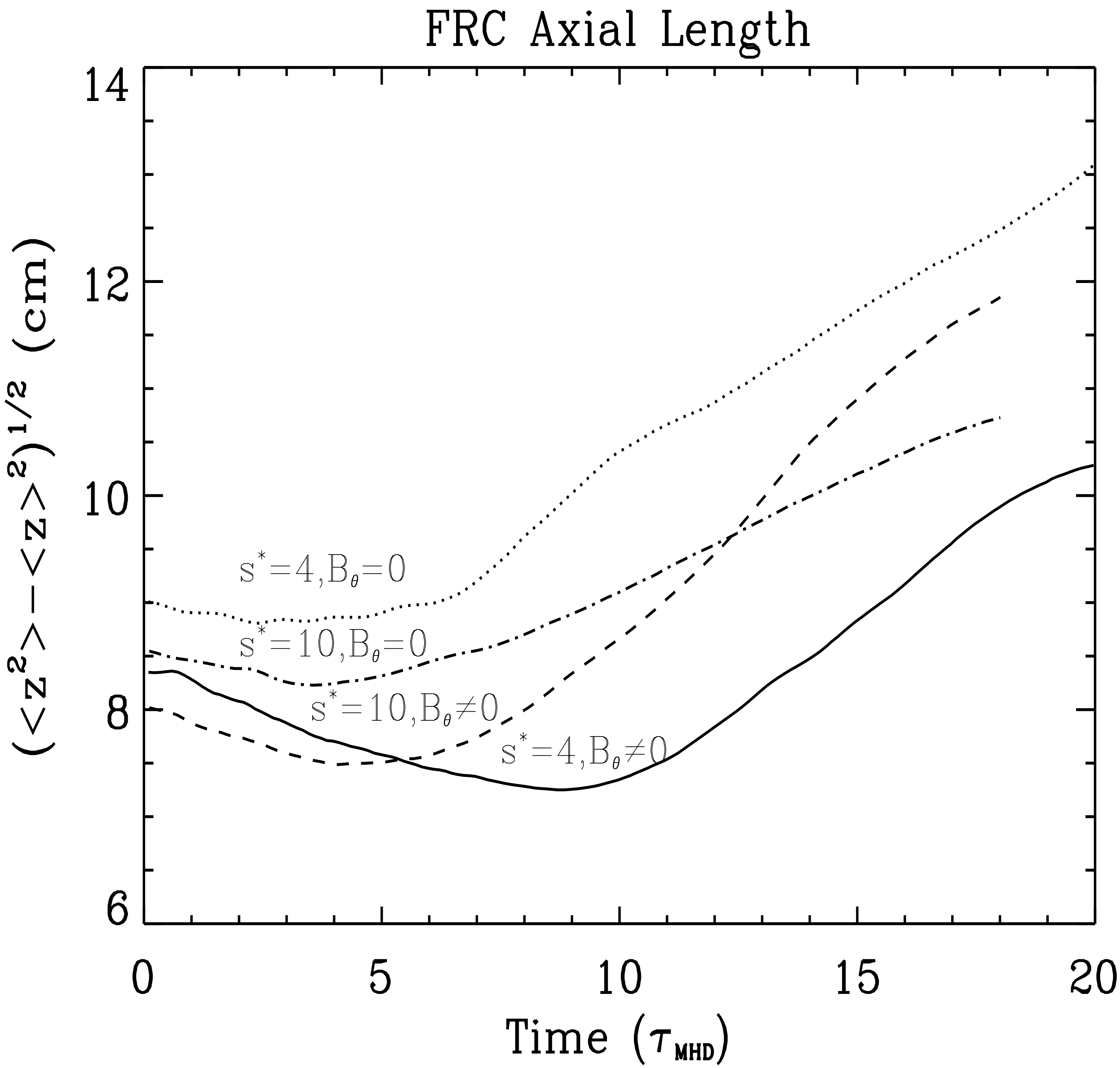

References

[1] Y.A. Omelchenko, Phys. Plasmas 7, 1443 (2000).

[2] Yu.A. Omelchenko and R.N. Sudan, J. Comp. Phys. 133, 146 (1997).

[3] L.C. Steinhauer, Phys. Plasmas 6, 2734 (1999).

[4] E.J. Horowitz, D.E. Shumaker, and D.V. Anderson, J. Comp. Phys. 84, 279 (1989).

[5] D.W. Hewett, Nucl. Fusion 24, 349 (1984).

[6] K. Wira and Z.A. Pietrzyk, Phys. Fluids B 2, 561 (1990).

[7] G. Durance and I.R. Jones, Phys. Fluids 29, 1196 (1986).

FIGURE CAPTIONS

Figure 1: Time evolution of the self-consistent kinetic FRC: (a) poloidal flux function ψ; (b) plasma density; (c) toroidal field.

Figure 2: Time evolution of the "zero-B_θ" kinetic FRC: (a) poloidal flux function ψ; (b) plasma density.

Figure 3: Time evolution of the self-consistent fluid-like FRC: (a) poloidal flux function ψ; (b) plasma density; (c) toroidal field.

Figure 4: Time evolution of the "zero-B_θ" fluid-like FRC: (a) poloidal flux function ψ; (b) plasma density.

Figure 5: Time histories of magnetic energy modes of the kinetic FRC: (a) poloidal field; (b) toroidal field; (c) $B_\theta = 0$.

Figure 6: Time histories of magnetic energy modes of the fluid-like FRC: (a) poloidal field; (b) toroidal field; (c) $B_\theta = 0$.

Figure 7: Time history of FRC plasma axial length evolution. The kink instability saturates through FRC axial expansion.